(±0.3) kcal mol^{-1}/RT] and those derived from our measured rate constants [log R = 0.6 (±0.2) + 0.9 (±0.7) kcal mol^{-1}/RT]. The values of R obtained from the two expressions agree exactly at 472 K and differ by 60% at 321 K.

Kinetics of the Reactions of Alkyl Radicals with Br_2. Each of the R + Br_2 reactions studied has a small negative activation energy (between −0.4 and −1.1 kcal mol^{-1}), indicating that there is no noticeable potential energy barrier along the reaction coordinate. The large values of the rate constants, k_1 to k_4, are consistent with a direct metathesis process of the repulsive type, the mechanism identified in the molecular beam investigations of reaction 1.[26-28] The insignificant secondary isotope effect observed for the CH_3 + Br_2 reaction at 298 K, $k(CD_3+Br_2)/k(CH_3+Br_2)$ = 1.16, is also in accord with this mechanistic picture.

Apparent negative activation energies could also have arisen in these experiments had undetected *bimolecular* R + Br_2 heterogeneous reactions been important because the relative importance of any heterogeneous processes of this sort would have been less at higher temperatures (where the degree of surface coverage by one or both reactants would be less). From our observations that the R + Br_2 rate constants are independent of the reactor wall coating used in the rate constant determinations (even when the coatings are chemically quite different), we have concluded that heterogeneous processes of this sort are not significant under our experimental conditions.

Kovalenko and Leone report an apparent enhancement in k_1 with increased translational energy of CH_3 which they state is due to a potential energy barrier along the reaction coordinate.[25] Our results do not support this explanation.

Hoffman et al.[28] indicate a small potential barrier in the entrance channel of the CH_3 + Br_2 reaction based solely on the fact that the value of k_1 reported by Kovalenko and Leone[25] corresponds to a thermally averaged cross section that is ≈1/10 that of the "hard-sphere cross section". Minor steric constraints in the dynamics of reaction 1 could also account for this difference.

All of the R + Br_2 reactions studied are very rapid processes, and differences in their rate constants are small. The four rate constants, k_1-k_4, have essentially the same Arrhenius A factor ((2.0-2.6) × 10^{-11}). That difference which is most apparent, the lower rate constant of reaction 1 compared with those of reactions 2-4, is due to the slightly higher (less negative) value of its activation energy.

A general picture is emerging of the kinetics of *exothermic* atom-transfer reactions between alkyl free radicals and halogen-containing diatomic molecules. There is generally no potential energy barrier along the reaction coordinate (activation energies are negative), and reactivity frequently runs counter to expectation based on reaction thermochemistry, i.e., opposite to the direction predicted by the Evans-Polanyi relationship.[34] This behavior has now been observed in the following series of alkyl radical reactions: R + Cl_2,[11] R + HI,[17] R + HBr,[13,14] and now R + Br_2.

For these and other atom-transfer reactions involving halogen-containing diatomic reactants,[35,36] reactivity correlates best with properties that reflect the magnitudes of long-range attractive forces, particularly those associated with the stabilization of intermediate states having some form of charge separation. These properties include the polarizability of the radical,[35] the ionization potential of the free radical,[11,36] and the difference between the ionization potential of one reactant and the electron affinity of the other.[37] The fact that these forces can determine reactivity trends while other reaction properties (such as overall reaction thermochemistry) could have produced the opposite trend in reactivity attests to the importance of these long-range forces. For reactions 1-4, the small differences in reactivity that do exist are consistent with this same mechanistic picture. The larger, more polarizable alkyl radicals react more rapidly than does the smallest (CH_3). The ordering in reactivity (k_1 < (k_2 to k_4)) is not that expected when considering only the influence of reaction thermochemistry.

Additional studies of the R + Br_2 reactions are in progress to learn more about the kinetics of these reactions.

Acknowledgment. This research was supported by funds from the National Science Foundation, Chemistry Division, under Grant CHE-8996126. We thank Dr. Irene R. Slagle for her advice, help, and support. J.A.S. thanks the Natural Science Council of the Academy of Finland and the Finnish Cultural Foundation for fellowships. R.S.T. thanks the Maj and Tor Nessling Foundation for financial support.

Registry No. CH_3, 2229-07-4; C_2H_5, 2025-56-1; i-C_3H_7, 2025-55-0; t-C_4H_9, 1605-73-8.

(34) (a) Evans, M. G.; Polanyi, M. *Trans. Faraday Soc.* **1938**, *34*, 11. (b) Evans, M. G.; Polanyi, M. *Trans. Faraday Soc.* **1936**, *32*, 1333.
(35) Krech, R. H.; McFadden, D. L. *J. Am. Chem. Soc.* **1977**, *99*, 8402.
(36) Loewenstein, L. M.; Anderson, J. G. *J. Phys. Chem.* **1985**, *89*, 5371.
(37) Loewenstein, L. M.; Anderson, J. G. *J. Phys. Chem.* **1987**, *91*, 2993.

Ammonia Activation by Sc^+ and Ti^+: Electronic and Translational Energy Dependence

D. E. Clemmer, L. S. Sunderlin, and P. B. Armentrout*,†

Department of Chemistry, University of Utah, Salt Lake City, Utah 84112 *(Received: August 30, 1989)*

The reactions of Sc^+ and Ti^+ with ammonia are studied as a function of translational energy in a guided ion beam tandem mass spectrometer. The effect of electronic energy for the Ti^+ reactions is also probed by varying the conditions for forming Ti^+. Excited doublet states of Ti^+ are found to be much more reactive than the a^4F ground and b^4F first excited states. Both metals form the MH^+, MNH^+, and MNH_2^+ products, while only Ti^+ forms MN^+. The results are consistent with reaction that occurs primarily through a covalently bound insertion intermediate, H-M^+-NH_2, having a singlet and doublet spin state for M = Sc and Ti, respectively. The reactivities of the different electronic states of the reactant ions can be explained by using spin conservation concepts. The thresholds for the cross sections of the endothermic reactions are interpreted to give the 298 K bond energies of $D°(Sc^+-NH_2)$ = 3.69 ± 0.07 eV, $D°(Sc^+-NH)$ = 5.16 ± 0.10 eV, $D°(Ti^+-NH_2)$ = 3.69 ± 0.13 eV, $D°(Ti^+-NH)$ = 4.83 ± 0.12 eV, and $D°(Ti^+-N)$ = 5.19 ± 0.13 eV. The large bond strengths of the M^+-NH_2 and M^+-NH species indicate that the lone pair electrons on the nitrogen atom are involved in the metal-ligand bond.

Introduction

Recent results from our laboratory have compared the reactions of V^+ with ammonia[1] to those with methane.[2] We find that while the reaction mechanisms are similar, the energetics of these systems are significantly different. The similarities observed in

† NSF Presidential Young Investigator, 1984-1989; Alfred P. Sloan Fellow; Camille and Henry Dreyfus Teacher-Scholar, 1988-1993.

(1) Clemmer, D. E.; Sunderlin, L. S.; Armentrout, P. B. *J. Phys. Chem.* **1990**, *94*, 208.
(2) Aristov, N.; Armentrout, P. B. *J. Phys. Chem.* **1987**, *91*, 6178-6188.

0022-3654/90/2094-3008$02.50/0

TABLE I: Heats of Formation and Bond Strengths for NH_n Species (298 K)[a]

neutral	$\Delta_f H°$, eV	bond	$D°$, eV
H	2.259 (0.0001)	N–H	3.45_5 (0.01_3)
N	4.899 (0.001)	HN–H	4.00_3 (0.01_6)
NH	3.70_3 (0.01_3)[b]	$HN–H_2$	4.17_9 (0.01_4)
NH_2	1.96 (0.01)[b]	$H_2N–H$	4.69_5 (0.01_4)
NH_3	−0.476 (0.004)	$D_2N–D$	4.81_3 (0.01_4)[c]

[a] All values except where noted are from ref 20. Uncertainties are in parentheses. [b] Derived from $\Delta_f H°_0$ results for NH and NH_2 in Anderson, W. R. *J. Phys. Chem.* **1989**, *93*, 530–536. [c] Reference 20 calculates that $D°(D_2N–D) > D°(H_2N–H)$ by 0.118 eV. Thus, we use this factor along with the revised ammonia thermochemistry to obtain $D°(D_2N–D)$.

reaction mechanisms were explained as a result of the fact that ammonia and methane are isoelectronic (in the sense that the central heavy atom has the same number of valence electrons with the same sp^3 hybridization).[3] Therefore, all products observed in the reaction of V^+ with ammonia have isoelectronic analogues to products formed in the V^+ with methane system. The differences in the energetics are attributed to the lone pair of electrons present on the nitrogen atom of ammonia but absent on the carbon atom of methane. Specifically, the lone pair was found to stabilize the VNH^+ and VNH_2^+ product molecules, leading to bond strengths for these products that are ~1.4 eV stronger than the isoelectronic methane analogues, VCH_2^+ and VCH_3^+. Presumably, this enhancement is a result of donation of the lone pair electrons into empty d orbitals on the metal ion.

In the present study, we extend this work by examining the interaction of ammonia with Sc^+ and Ti^+. In both cases, the reaction of the ion with methane has been studied previously.[4,5] Because Sc^+ and Ti^+ have fewer d electrons than V^+, there are again empty d orbitals accessible to lone pair donation, and thus, we anticipate similar behavior to that found in the V^+ with ammonia experiment.

The exothermic interactions of Sc^+ and Ti^+ with ammonia have been studied previously by using Fourier transform ion cyclotron resonance (FTICR) mass spectrometry by Buckner, Gord, and Freiser (BGF).[6] In both cases, they observe the exothermic formation of MNH^+ as the only reaction at thermal energies. These results indicate that $D°(Sc^+–NH)$ and $D°(Ti^+–NH) \geq D°(NH–H_2) = 4.18 \pm 0.01$ eV, Table I (assuming that ground-state ions are responsible for the observed reactivity). In the present guided ion beam studies, a detailed investigation over an extended kinetic energy range is performed. Thus, endothermic processes, as well as those exothermic ones, are probed. In addition, we distinguish between the reactivities of specific electronic states of the titanium ion. This allows us to also examine the electronic requirements for the reactions observed. In the case of V^+, the excited triplet states are about 2 orders of magnitude more reactive with ammonia than the low-lying quintet states. This result was rationalized by using molecular orbital and spin conservation concepts.[1]

Experimental Section

General. Complete descriptions of the apparatus and experimental procedures are given elsewhere.[7] Sc^+ and Ti^+ production is described below. The ions are extracted from the source, accelerated, and focused into a magnetic sector momentum analyzer for mass analysis. Mass-selected ions are slowed to a desired kinetic energy and focused into an octopole ion guide which radially traps the ions. The octopole passes through a static gas cell containing the neutral reactant. Ammonia[8] pressures in the cell are kept low (~0.1 mTorr) so that multiple ion–molecule collisons are improbable. Product and unreacted beam ions are contained in the guide until they drift out of the gas cell where they are focused into a quadrupole mass filter for mass analysis and then detected. Ion intensities are converted to absolute cross sections as described previously.[7] Uncertainties in cross sections are estimated to be ±20%.

TABLE II: Sc^+ and Ti^+ Beam Populations

				% population[b]			
ion	state	confign	E,[a] eV	1950 K	2225 K	2400 K	30 eV
Sc^+	a^3D	4s3d	0.013		88.0	86.4	
	a^1D	4s3d	0.315		6.1	6.7	
	a^3F	$3d^2$	0.608		5.5	6.8	
	b^1D	$3d^2$	1.357		<0.1	<0.1	
Ti^+	a^4F	$3d^24s$	0.028	64.56	62.31	61.04	73 (7)[c]
	b^4F	$3d^3$	0.135	34.14	35.66	36.39	
	a^2F	$3d^24s$	0.593	1.12	1.64	1.98	9 (3),[c] 14 (5)[d]
	a^2D	$3d^24s$	1.082	0.04	0.09	0.13	
	a^2G	$3d^3$	1.124	0.06	0.13	0.20	
	a^4P	$3d^3$	1.172	0.03	0.07	0.10	
	a^2P	$3d^3$	1.232	0.01	0.02	0.04	
	b^4P	$3d^24s$	1.236	0.02	0.05	0.08	
	others		≥1.575	<0.01	<0.02	<0.05	
	∑states > 0.5 eV			1.29	2.02	2.58	

[a] Energies are a statistical average over the J levels. [b] Maxwell–Boltzmann distribution. [c] Estimates from ref 5. [d] Average estimates from the populations extracted from the TiN^+, $TiNH^+$, and $TiNH_2^+$ channels given in text.

Laboratory ion energies relate to center-of-mass (CM) frame energies by $E_{CM} = E_{lab}m/(M + m)$, where M and m are the ion and neutral reactant masses, respectively. Below ≈0.3 eV lab, energies are corrected for truncation of the ion beam energy distribution as described previously.[7] Absolute energy scale uncertainties are ±0.05 eV lab.[9] Two effects broaden the data: the ion energy spread, which is independent of energy and has a fwhm of ~0.7 eV lab, and thermal motion of the neutral gas, which has a width of $\sim 0.46E_{CM}^{1/2}$ for these reactions.[10]

Ion Sources. Sc^+ and Ti^+ are produced by surface ionization (SI). In the SI source, the metal is introduced to the gas phase as $TiCl_4$ (Aldrich, 99.9%) vapor or by vaporizing $ScCl_3·6H_2O$ (Aesar) in an oven. The metal halide vapor is directed toward a resistively heated rhenium filament where it decomposes, and the resulting metal atoms are ionized. It is generally assumed that ions produced by SI equilibrate at the temperature of the filament and the state populations are governed by a Maxwell–Boltzmann distribution. The validity of this assumption has been discussed previously.[5] Table II lists the energies and populations of states for Sc^+ and Ti^+ produced at the SI temperatures used in these experiments. Since all transitions between states in Table II are parity forbidden, the radiative lifetimes of the excited states (on the order of seconds long)[11] are expected to be much greater than the flight time between the ionization and reaction regions (~10–100 μs). Thus, very few excited ions radiatively relax before reaction. Ti^+ is also produced by electron impact (EI) of $TiCl_4$ vapor. Here, the state populations are not characterized by a Maxwellian distribution since vertical processes dominate ionization.

Thermochemical Analyses. Theory[12,13] and experiment[2,14–16]

(3) Bent, H. A. *J. Chem. Educ.* **1966**, *43*, 170–186.
(4) Sunderlin, L. S.; Armentrout, P. B. *J. Am. Chem. Soc.* **1989**, *111*, 3845–3855.
(5) Sunderlin, L. S.; Armentrout, P. B. *J. Phys. Chem.* **1988**, *92*, 1209–1219.
(6) Buckner, S. W.; Gord, J. R.; Freiser, B. S. *J. Am. Chem. Soc.* **1988**, *110*, 6606–6612.
(7) Ervin, K. M.; Armentrout, P. B. *J. Chem. Phys.* **1985**, *83*, 166–189.
(8) Before usage, NH_3 (Matheson, 99.99%) and $^{14}ND_3$ (Cambridge Isotope Laboratories, 99.5%) were subjected to multiple freeze–pump–thaw cycles with liquid nitrogen to remove volatile impurities.
(9) Burley, J. D.; Ervin, K. M.; Armentrout, P. B. *Int. J. Mass Spectrom. Ion Processes* **1987**, *80*, 153–175.
(10) Chantry, P. J. *J. Chem. Phys.* **1971**, *55*, 2746–2759.
(11) Garstang, R. H. *Mon. Not. R. Astron. Soc.* **1962**, *124*, 321; personal communication.
(12) See discussion in: Aristov, N.; Armentrout, P. B. *J. Am. Chem. Soc.* **1986**, *108*, 1806–1819.
(13) Chesnavich, W. J.; Bowers, M. T. *J. Phys. Chem.* **1979**, *83*, 900–905.
(14) Armentrout, P. B.; Beauchamp, J. L. *J. Chem. Phys.* **1981**, *74*, 2819–2826. Armentrout, P. B.; Beauchamp, J. L. *J. Am. Chem. Soc.* **1981**, *103*, 784–791.

indicate that the cross sections for endothermic reactions can be analyzed by using eq 1, which involves an explicit sum of the

$$\sigma(E) = \sum_i g_i \sigma_0 (E - E_0 + E_i)^n / E \quad (1)$$

contributions of individual states, denoted by i, weighted by their populations, g_i. Here, σ_0 is a scaling factor, E is the relative kinetic energy, n is an adjustable parameter, E_0 is the threshold for reaction of the lowest electronic level of the ion [$J = 1$ for $Sc^+(a^3D)$ and $J = 3/2$ for $Ti^+(a^4F)$], and E_i is the electronic excitation of each particular J level (for convenience, these are the J-averaged values for Sc^+ and Ti^+ given in Table II). The σ_0, n, and E_0 parameters are optimized by using a nonlinear least-squares analysis to give the best fit to the data, after convoluting over the neutral and ion kinetic energy distributions as described previously.[7] Error limits for E_0 are calculated from the range of threshold values for different data sets and the absolute energy scale error.

For ion beams produced by EI, the distribution of electronic states present is unknown. In such cases, analysis with eq 1 cannot include an explicit summation over states, and the result is an average threshold energy E_T. The difference between E_T and E_0 (determined from the SI data sets) allows a determination of E_{el}, the average electronic energy of the beam.

Some data channels also require a modified form of eq 1 which accounts for dissociation of the product ion at higher energies. This model has been described in detail previously[17] and depends on E_D, the energy at which a dissociation channel or a competing reaction can begin.

Assuming that E_0 is the enthalpy difference between reactants and products allows us to calculate the metal–ligand bond energies. This implies that activation barriers are smaller than the endothermicity, an assumption which is often true for ion–molecule reactions.[18] We also assume that the ammonia and the products formed at the threshold of an endothermic reaction are characterized by a temperature of 298 K in all degrees of freedom. Thus, we make no correction for the energy available in internal modes of the neutral reactant.

Results

The reaction of Sc^+ with ND_3 yields three products:

$$Sc^+ + ND_3 \rightarrow ScD^+ + ND_2 \quad (2)$$

$$\rightarrow ScND^+ + D_2 \quad (3)$$

$$\rightarrow ScND_2^+ + D \quad (4)$$

Ti^+ reacts with ND_3 to form four products:

$$Ti^+ + ND_3 \rightarrow TiD^+ + ND_2 \quad (5)$$

$$\rightarrow TiN^+ + D_2 + D \quad (6)$$

$$\rightarrow TiND^+ + D_2 \quad (7)$$

$$\rightarrow TiND_2^+ + D \quad (8)$$

Figures 1 and 2 show the cross sections for these reactions when Sc^+ and Ti^+ are produced at a filament temperature of 2225 K. Cross sections for reaction of Sc^+ and Ti^+ with NH_3 are similar

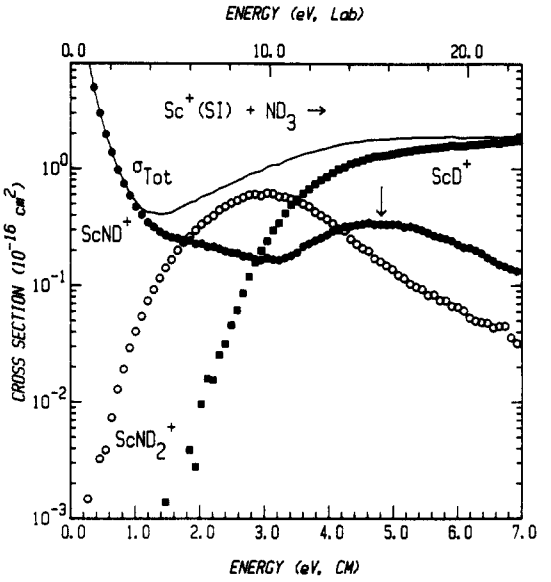

Figure 1. Variation of product cross sections for reaction of ND_3 with Sc^+ produced by SI at 2225 K as a function of translational energy in the center-of-mass frame (lower scale) and laboratory frame (upper scale). The solid line is the sum of the cross sections for all products. The arrow at 4.81 eV shows the bond energy $D°(D_2N–D)$.

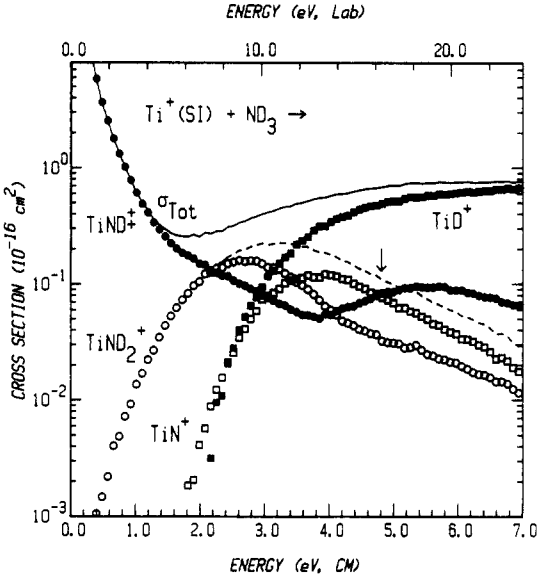

Figure 2. Variation of product cross sections for reaction of ND_3 with Ti^+ produced by SI at 2225 K as a function of translational energy in the center-of-mass frame (lower scale) and laboratory frame (upper scale). The solid line is the sum of the cross sections for all products. The dashed line is the sum of $\sigma(TiN^+)$ and $\sigma(TiND_2^+)$. The arrow at 4.81 eV shows the bond energy $D°(D_2N–D)$.

to those shown in Figures 1 and 2.[19] As observed by BGF, the dominant process at thermal energies for reaction of both ions is dehydrogenation, reactions 3 and 7. The fact that $\sigma(ScND^+)$ and $\sigma(TiND^+)$ increase with decreasing energy to as low an energy as we can measure (~0.03 eV) indicates that reactions 3 and 7 are exothermic. This means that formation of $ScND^+$ and $TiND^+$

(15) Boo, B. H.; Armentrout, P. B. *J. Am. Chem. Soc.* **1987**, *109*, 3549–3559.
(16) Sunderlin, L.; Aristov, N.; Armentrout, P. B. *J. Am. Chem. Soc.* **1987**, *109*, 78–89.
(17) Weber, M. E.; Elkind, J. L.; Armentrout, P. B. *J. Chem. Phys.* **1986**, *84*, 1521–1529.
(18) Boo, B. H.; Armentrout, P. B. *J. Am. Chem. Soc.* **1987**, *109*, 3549–3559. Ervin, K. M.; Armentrout, P. B. *J. Chem. Phys.* **1986**, *84*, 6738–6749. Ervin, K. M.; Armentrout, P. B. *J. Chem. Phys.* **1987**, *86*, 2659–2673. Elkind, J. L.; Armentrout, P. B. *J. Phys. Chem.* **1984**, *88*, 5454–5456.

(19) ND_3 results are shown in Figures 1 and 2 due to small contributions in the titanium system from the exothermic reaction of Ti^+ with O_2 contaminant. In the ND_3 system, the TiO^+ product has the same mass as the large $TiND^+$ product and therefore makes a negligible contribution. In the NH_3 system, the TiO^+ product has the same mass as $TiNH_2^+$, which has a small cross section at low kinetic energies for the SI data. Thus, even minor amounts of TiO^+ can affect the appearance of the $TiNH_2^+$ cross section. In the detailed analysis of both the Sc^+ and Ti^+ reactions, the $M^+ + NH_3$ data are preferred, except for reactions 4 and 8, where both $\sigma(MND_2^+)$ and $\sigma(MNH_2^+)$ are examined.

must produce the stable D_2 molecule. Further evidence for D_2 production is that $\sigma(ScND^+)$ and $\sigma(TiND^+)$ also exhibit endothermic features having apparent onsets of ~3 and ~4 eV, respectively. These features must be due to reactions 9 and 10, respectively, which are 4.6 eV = $D°(D_2)$ more endothermic than reactions 3 and 7.[20]

$$Sc^+ + ND_3 \rightarrow ScND^+ + D + D \quad (9)$$

$$Ti^+ + ND_3 \rightarrow TiND^+ + D + D \quad (10)$$

The cross sections for $ScND_2^+$ and $TiND_2^+$ peak between 2.5 and 3.0 eV. This behavior cannot be due to dissociation to $M^+ + ND_2$ since this requires 4.81 eV, Table I. Other dissociation pathways for MND_2^+ are loss of D, reactions 9 and 10, and loss of D_2, which only occurs for Ti^+, reaction 6. For Sc^+, reaction 9 accounts for some of the decline in $\sigma(ScND_2^+)$, but the sum of these cross sections still peaks before 4.81 eV. Likewise, the sum of the cross sections for reactions 6, 8, and 10 also declines well before this energy. Thus, other processes cannot fully account for the early decline observed in the MND_2^+ cross section. The remaining explanation is that $\sigma(MND_2^+)$ is influenced by formation of MD^+, reactions 2 and 5, the dominant product channel at high energies. Competition between these two channels is consistent with the smooth appearance of the total cross sections for both sets of reactions. For reaction of V^+ with ammonia,[1] competition between formation of VH^+ and VNH_2^+ accounted for the early peak position of VNH_2^+.

For the case of Ti^+, the metal nitride product, reaction 7, can be formed via D_2 loss from $TiND_2^+$, as noted above, or by D atom loss from $TiND^+$. The small magnitude of $\sigma(TiND^+)$ at energies where TiN^+ is formed and the smooth falloff of the $\sigma(TiND_2^+) + \sigma(TiN^+)$ sum suggest that the major portion of $\sigma(TiN^+)$ comes from the $TiND_2^+$ precursor.

One final point of interest concerns the relative magnitudes of the cross sections for reactions 9 and 10. While the magnitudes of the exothermic features of $\sigma(ScND^+)$ and $\sigma(TiND^+)$ are similar, Figures 1 and 2, the magnitude of $\sigma(ScND^+)$ formed endothermically is much greater than that for $\sigma(TiND^+)$. We believe this is because the decomposition of MND_2^+ to form $MN^+ + D_2$ does not occur for Sc^+ but does for Ti^+. Thus, while there is a competition between forming TiN^+ and $TiND^+$ from decomposition of $TiND_2^+$, since $ScND_2^+$ does not decompose to ScN^+, the production of $ScND^+$ is noticeably enhanced at higher energies.

Data Analysis

Determination of Spin-Specific Cross Sections. As mentioned above, the electronic-state composition of the V^+ beam used in the reaction of V^+ with ammonia was found to greatly affect the reaction cross sections.[1] Thus, it is of interest to determine the electronic-state dependence of the reactions of both Sc^+ and Ti^+ with ammonia. In the case of Sc^+, we are only able to produce ions by SI at filament temperatures between 2225 and 2400 K. Over this temperature range, we observe no changes in the ammonia cross sections. However, this range of temperatures leads to only small changes in the populations of excited states (Table II). This makes the temperature study inconclusive concerning the role of excited-state Sc^+ (although it does establish that the observed reactivity is dominated by ground-state, not excited-state, Sc^+).

For Ti^+, previous experiments in our laboratory with H_2[21] and methane[5] have shown that excited doublet states of Ti^+ react much more efficiently than the low-lying a^4F and b^4F states. For larger alkanes, the effect is substantially muted.[22] As in these previous studies, we can use variations in the reaction cross sections with source conditions to extract state-specific cross sections here.

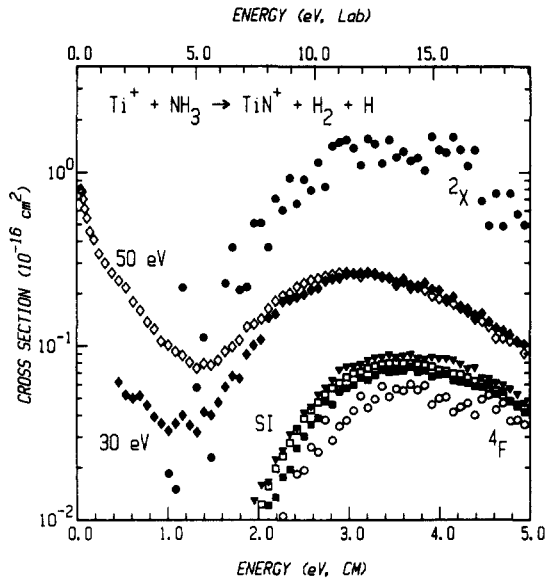

Figure 3. Kinetic energy dependence of $\sigma(TiN^+)$ formed by reaction of NH_3 with Ti^+ produced by SI at 1950 K (■), by SI at 2225 K (□), by SI at 2400 K (▼), by EI at 30 eV (♦), and by EI at 50 eV (◇) as a function of translational energy in the laboratory frame (upper axis) and the center-of-mass frame (lower axis). $\sigma(^4F)$ (○) and $\sigma(^2X)$ (●) extrapolated from the SI data, see text, are also shown.

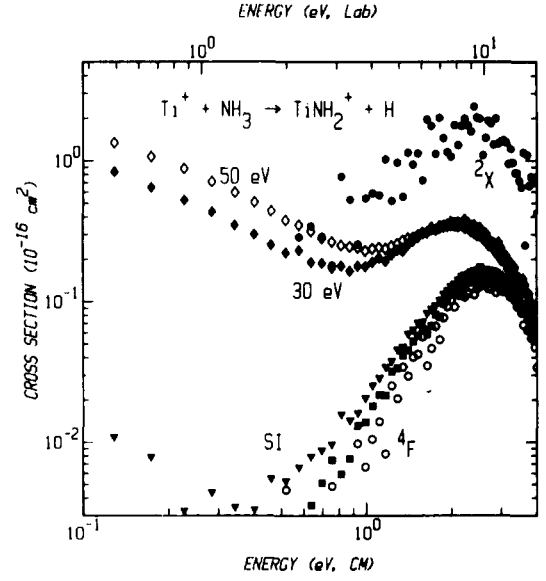

Figure 4. Kinetic energy dependence of $\sigma(TiNH_2^+)$ formed by reaction of NH_3 with Ti^+ produced by EI at 30 eV (♦) and 50 eV (◇) as a function of translational energy in the laboratory frame (upper axis) and the center-of-mass frame (lower axis). Kinetic energy dependence of $\sigma(TiND_2^+)$ formed by reaction of ND_3 with Ti^+ produced by SI at 1950 K (■) and 2400 K (▼) as a function of translational energy in the center-of-mass frame (lower axis). Also shown are the ^4F (○) and ^2X (●) cross sections extrapolated from the SI cross sections.

Figures 3 and 4 show that there is a small but reproducible increase in the cross sections for TiN^+ and $TiND_2^+$ as the SI filament temperature is increased from 1950 to 2225 to 2400 K. This increase in filament temperature leads to cross sections for both products which increase in ratios of 1.0:1.5:2.2 at energies which are near the apparent threshold for the 1950 K data (1.9 eV for TiN^+ and 0.5 eV for TiN_2^+). Table II shows that for these temperatures the population of the a^4F state decreases, while that for the b^4F state increases in ratios of only 1.00:1.04:1.07. Thus, the changes observed cannot be explained by reaction of the quartet states. On the other hand, the a^2F state increases in ratios of 1.0:1.5:1.8, while higher lying states increase as 1.0:2.2:3.5. The sum of the a^2F and higher excited-state populations increases as

(20) Chase, M. W.; Davies, C. A.; Downey, J. R.; Frurip, D. J.; McDonald, R. A.; Syverud, A. N. *J. Phys. Chem. Ref. Data* **1985**, *14* (Suppl. No. 1) (JANAF Tables).

(21) Elkind, J. L.; Armentrout, P. B. *Int. J. Mass Spectrom. Ion Processes* **1988**, *83*, 259–284.

(22) Sunderlin, L. S.; Armentrout, P. B. *Int. J. Mass Spectrom. Ion Processes* **1989**, *94*, 149–177.

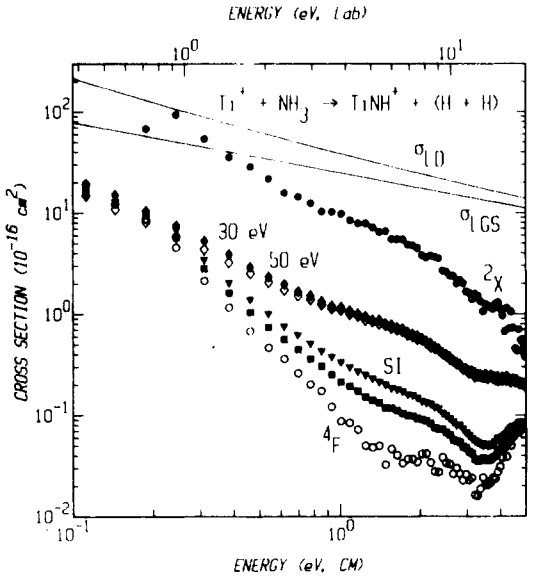

Figure 5. Kinetic energy dependence of $\sigma(TiNH^+)$ formed by reaction of ammonia with Ti^+ produced by SI at 1950 K (■) and 2400 K (▼) and by EI at 30 eV (♦) and at 50 eV (◇) as a function of translational kinetic energy in the laboratory frame (upper axis) and the center-of-mass frame (lower axis). The ^4F (○) and ^2X (●) cross sections extrapolated from the SI data, see text, are also shown. Full lines show the theoretical collision cross sections, σ_{LGS} and σ_{LD}.

1.0:1.6:2.0. Clearly, the change in cross section with filament temperature can be attributed to these excited states and largely the a^2F. Therefore, we use a sum of the populations of these states to linearly extrapolate the 1950, 2225, and 2400 K cross sections at each kinetic energy to cross sections containing 0.0% or 100% of these excited states. The former extrapolation yields cross sections due to reaction of a^4F and b^4F ions (referred to, henceforward, as ^4F, since the individual a^4F and b^4F state reactivities cannot be unambiguously determined). The latter cross section is from reaction of the higher energy states (denoted ^2X, since doublet states and the a^2F, in particular, dominate the population, Table II). These extrapolated cross sections are shown in Figures 3 and 4. The same method is used to generate spin-specific cross sections for the $TiNH^+$ data channel, Figure 5. For TiH^+, no clear filament temperature dependence exists, and therefore no extrapolations were performed.

Comparison of $\sigma(^4F)$ and $\sigma(^2X)$ in the TiN^+ channel indicates that the latter states are 16 ± 8 times more reactive than the former, even after accounting for the available energy. The same comparison for the $TiNH_2^+$ channel shows that the ^2X states are more reactive than the ^4F states by a factor of 7 ± 3. For the $TiNH^+$ channel, the relative reactivities vary strongly with energy such that ratio starts at ~10 at low energies (~0.2 eV) but then increases up to 1 eV where it remains at 100 ± 30 until about 3 eV.

MH^+. The most efficient process for the reaction of Sc^+ and Ti^+ with ammonia at energies above ~2.5 eV is production of MH^+. The best fit to $\sigma(ScH^+)$ using eq 1, the state populations of Table II, and the parameters given in Table III, gives E_0 = 2.36 ± 0.09 eV. Combining E_0 with $D°(NH_2–H)$, Table I, yields $D°(ScH^+)$ = 2.33 ± 0.09, in agreement with our previously reported ScH^+ bond energy of 2.48 ± 0.09 eV.[23] This agreement implies that eq 1 adequately accounts for the excited-state contributions to $\sigma(ScH^+)$ and that there are no substantive barriers in excess of the reaction endothermicity.

Figure 6 shows $\sigma(TiH^+)$ produced by SI at 1950 K and EI at electron energies of 30 and 50 eV. The reaction is sensitive to the Ti^+ production conditions, as shown by the different shapes and magnitudes of the cross sections. The increased magnitude and lower threshold displayed by the EI data, when compared

(23) Elkind, J. L.; Sunderlin, L. S.; Armentrout, P. B. *J. Phys. Chem.* **1989**, *93*, 3151–3158.

TABLE III: Summary of Parameters of Eq 1 Used To Fit Threshold

product ion	ion source[a]	E_T, eV	σ_0	n
ScH^+	SI, 2225 K	2.36 ± 0.09	2.1 ± 0.6	1.2 ± 0.1
$ScNH^+$	SI, 2225 K	3.54 ± 0.10	1.4 ± 0.3	=1.0
$ScNH_2^+$	SI, 2225 K	1.01 ± 0.07	0.7 ± 0.2	1.8 ± 0.2
$ScND_2^+$	SI, 2225 K	1.10 ± 0.07	1.0 ± 0.1	1.8 ± 0.2
TiH^+	SI, 1950 K	2.40 ± 0.12	1.2 ± 0.3	1.0 ± 0.1
	EI, 30 eV	2.02 ± 0.15	2.5 ± 0.2	1.0 ± 0.1
	EI, 50 eV	1.90 ± 0.10	2.2 ± 0.2	1.1 ± 0.1
TiN^+	^4F	2.44 ± 0.12	0.2 ± 0.1	1.0 ± 0.1
	EI, 30 eV	1.75 ± 0.08	0.5 ± 0.1	=1.0
	EI, 50 eV	1.63 ± 0.07	0.6 ± 0.1	=1.0
$TiNH^+$	^4F	3.87 ± 0.12	0.4 ± 0.1	=1.0
$TiND_2^+$	^4F	1.12 ± 0.13	0.2 ± 0.1	1.8 ± 0.2
	^2X	0.30 ± 0.15	1.0 ± 0.3	2.1 ± 0.3

[a] This refers to the M^+ source used to obtain the raw data analyzed. In cases where the ^4F or ^2X state is referred to, the text provides a complete description of the derivation of the cross section analyzed.

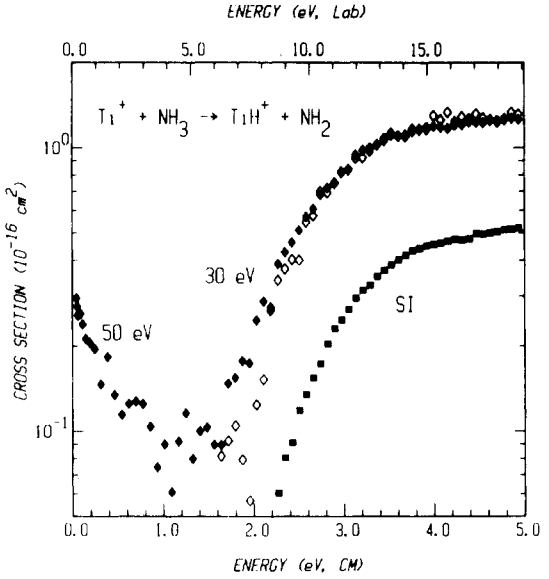

Figure 6. Kinetic energy dependence of $\sigma(TiH^+)$ formed by reaction of NH_3 with Ti^+ produced by SI at 1950 K (■), by EI at 30 eV (♦), and by EI at 50 eV (◇) as a function of translational energy in the laboratory frame (upper axis) and the center-of-mass frame (lower axis).

to the SI data, indicates that more than one electronic state can form TiH^+. Fitting the cross sections arising from 1950 K SI data sets with eq 1, populations from Table II, and the parameters given in Table III gives a threshold for TiH^+ formation of 2.40 ± 0.12 eV. Combined with $D°(NH_2–H)$, this value yields $D°(Ti^+–H)$ = 2.30 ± 0.12 eV, in agreement with our previously reported value, 2.35 ± 0.11 eV.[21]

The 30-eV cross section shown in Figure 3 is about a factor of 3 larger than the SI cross sections and is nonzero (~10^{-18} cm^2) at the lowest energies we can measure. Analysis of the endothermic feature of this cross section using eq 1 and the fitting parameters (Table III) gives E_T = 2.02 ± 0.15 eV, 0.38 ± 0.19 eV lower than E_0. This is consistent with the a^2F (E_{el} = 0.59 eV) state being the major contributor to the 30-eV cross section.

The 50-eV EI cross section shows an exothermic as well as an endothermic feature for TiH^+ production. The endothermic feature has the same ~2.0-eV onset and magnitude as the 30-eV cross section. The exothermicity of the 50-eV cross section indicates that ions with at least 2.3 eV of electronic energy are populated in this beam. Increasing the electron energy to 70 eV yields a cross section almost identical with that obtained from the 50-eV beam.

MN^+. Formation of ScN^+ does not occur within the detection limits of this experiment (~10^{-19} cm^2); however, TiN^+ formation occurs readily, Figure 3. Comparison of the extrapolated ^4F cross section with the SI data shows that the data are dominated by reaction of the ^4F states of Ti^+. Analysis of the ^4F cross section

(using eq 1, the populations of the two low-lying ^4F states, and the fitting parameters given in Table III) gives $E_0 = 2.44 \pm 0.12$ eV and $E_D = 4.01 \pm 0.16$ eV. Combining E_0 with the thermochemistry in Table I leads to $D°(Ti^+–N) = 5.19 \pm 0.13$ eV.

Figure 4 also shows $\sigma(TiN^+)$ obtained by using the EI source, at electron energies of 30 and 50 eV. Cross sections obtained at 70 eV are nearly identical with those obtained at 50 eV. All EI cross sections display exothermic as well as endothermic features. The endothermic features are greater in magnitude and have lower thresholds than the SI cross sections. Fitting the exothermic feature of the 30-eV cross section with a power law ($0.38E^{-0.6}$) and subtracting this from the cross section leaves an endothermic feature which has the same shape as $\sigma(^2X)$. Analysis of this feature by eq 1, Table III, yields $E_T = 1.75 \pm 0.08$ eV and $E_D = 3.50 \pm 0.09$ eV. These values are lower than those for reaction of the ^4F states by 0.69 ± 0.15 and 0.51 ± 0.18 eV, respectively. This threshold and peak shift correspond to the a^2F excitation energy, $E_{el} = 0.59$ eV, and suggest that this state is responsible for the endothermic feature of the 30-eV $\sigma(TiN^+)$. These shifts further verify the a^2F state as the major contributor to the extrapolated ^2X state cross section. The exothermic feature of the 30-eV cross section indicates that states with $E_{el} \geq 2.35$ eV also contribute to the reaction cross section. However, the small magnitude indicates that these ions make up only a small percentage of the 30-eV beam.

The 50-eV cross section is similar to the 30-eV cross section at high energies. However, the exothermic feature of this cross section is much larger than that for the 30-eV beam. This indicates that an even greater portion of the beam is made up of ions with $E_{el} \geq 2.35$ eV. Subtracting a power law fit to the exothermic feature ($0.10E^{-1.2}$) from the 50-eV cross section, and analyzing the resulting cross section with eq 1, Table III, gives $E_T = 1.63 \pm 0.07$ eV and $E_D = 3.38$ eV. Again, the threshold and peak energies for this feature correspond most closely to contributions from the a^2F state.

MNH^+. Figure 5 shows the ^4F and ^2X extrapolated cross sections for $TiNH^+$. These demonstrate that this product is formed exothermically for both quartet and doublet spin states. The exothermicity of the former state sets a lower limit to $D°(Ti^+–NH)$ of 4.18 eV = $D°(HN–H_2)$, Table I. A more precise value of this bond energy can be obtained by analyzing the cross section for reaction 10, the endothermic feature of $\sigma(^4F)$. We arrive at the threshold for this feature by fitting the ^4F cross section in the energy region below the endothermic feature (between ~2.3 and 3.3 eV) with a power law and subtracting this fit from $\sigma(TiNH^+,^4F)$. This process leaves only the endothermic feature which upon analysis with eq 1, the populations of the a^4F and b^4F states, and the fitting parameters listed in Table III gives $E_0 = 3.87 \pm 0.12$ eV. Since the bond energy of H_2 is 4.52 eV, this threshold is consistent with the exothermicity of reaction 7 (for NH_3) for ground-state ions. Combining E_0 with the thermochemistry of Table I gives $D°(Ti^+–NH) = 4.83 \pm 0.12$ eV. The threshold for reaction 9 can be analyzed in a similar manner, Table III, and yields $E_0 = 3.54 \pm 0.10$ eV, leading to $D°(Sc^+–NH) = 5.16 \pm 0.10$ eV.

Figure 5 also shows $TiNH^+$ cross sections obtained from EI beams produced at 30 and 50 eV. These cross sections decline more slowly with increasing energy ($E^{-1.0\pm0.1}$) than the SI cross sections ($E^{-1.7\pm0.1}$). Further, the EI cross sections display no obvious endothermic feature (due to reaction 10) as observed in the SI cross sections. Presumably, the larger magnitude of the exothermic process in the EI cross sections masks the smaller endothermic process (which might exhibit itself as the break in cross section slope at ~3 eV, Figure 5).

MNH_2^+. Cross sections obtained for the reaction of Sc^+ produced by SI at 2225 K with NH_3 (ND_3) to form $ScNH_2^+$ ($ScND_2^+$) are analyzed by using eq 1, the populations and energies of the states of the reactant ion beam (Table II), and the fitting parameters listed in Table III. This analysis gives E_0 and E_D for $\sigma(ScNH_2^+)$ as 1.01 ± 0.07 and 2.82 ± 0.17 eV, respectively. E_0 and E_D for $\sigma(ScND_2^+)$ are 1.10 ± 0.07 and 3.13 ± 0.14 eV, respectively. Combining these E_0 values with the thermochemistry from Table I gives $D°(Sc^+–NH_2) = 3.69 \pm 0.07$ eV and $D°(Sc^+–ND_2) = 3.71 \pm 0.08$ eV.

TABLE IV: Heats of Formation and Bond Dissociation Energies (eV) at 298 K

$M^+–L$	$\Delta_fH°(ML^+)^a$	$D°(M^+–L)^b$	$D°(CH_n–L)^c$
ScH^+	10.32 (0.12)	2.48 (0.09)[d]	4.55 (0.02)
		2.33 (0.09)	
TiH^+	11.71 (0.13)	2.35 (0.11)[e]	
		2.30 (0.12)	
TiN^+	11.51 (0.15)	5.19 (0.13)	9.66 (0.20)
$ScNH^+$	9.08 (0.13)	5.16 (0.10)	6.32 (0.16)
$TiNH^+$	10.67 (0.14)	4.83 (0.12)	
$ScNH_2^+$	8.81 (0.10)	3.69 (0.07)	3.72 (0.02)
$TiNH_2^+$	10.06 (0.15)	3.69 (0.13)	
$TiCH^+$	12.71 (0.18)	5.25 (0.17)	9.95 (0.18)
$ScCH_2^+$	10.28 (0.25)	4.27 (0.23)	7.47 (0.06)
$TiCH_2^+$	11.76 (0.17)	4.05 (0.15)	
$ScCH_3^+$	9.49 (0.15)	2.56 (0.13)	3.89 (0.02)
$TiCH_3^+$	10.82 (0.14)	2.49 (0.12)	

[a] $\Delta_fH°$ for ions are calculated by using the thermal electron convention. $\Delta_fH°(Sc^+) = 10.54 \pm 0.08$ eV from Wagman et al. *J. Phys. Chem. Ref. Data* **1982**, *11* (Suppl. 2), and $\Delta_fH°(Ti^+) = 11.797 \pm 0.065$ eV.[20] [b] Values are from this study unless otherwise noted. [c] Bond energies are calculated by using $\Delta_fH°$ values from ref 20 and Pedley, J. B.; Naylor, R. D.; Kirby, S. P. *Thermochemical Data of Organic Compounds*, 2nd ed.; Chapman and Hall: London, 1986. The only exception is $\Delta_fH°(CH_2NH) = 32 \pm 2$ kcal/mol, taken from Lias, S. G.; Bartmess, J. E.; Liebman, J. F.; Holmes, J. L.; Levin, R. D.; Mallard, W. G. *J. Phys. Chem. Ref. Data* **1988**, *17* (Suppl. 1). [d] Reference 23. [e] Reference 21.

Figure 4 shows that the extrapolated ^4F cross section for reaction 8 is clearly endothermic. Analysis using eq 1 with the a^4F and b^4F state populations and the fitting parameters given in Table III yields $E_0 = 1.12 \pm 0.13$ eV and $E_D = 2.67 \pm 0.08$ eV. Combining E_0 with $D°(ND_2–D)$ gives $D°(TiND_2^+) = 3.69 \pm 0.13$ eV. Since $D°(ScNH_2^+) \approx D°(ScND_2^+)$, we assume that $D°(TiND_{2+}) \approx D°(TiNH_2^+) = 3.69 \pm 0.13$ eV, which is the bond strength we report.

The extrapolated ^2X cross section is dominated by a process that is endothermic but does not go to zero at our lowest energies. This is consistent with the E_0 value of 1.12 eV, since this predicts that the a^2F state reaction should be endothermic by 0.53 ± 0.13 eV while higher lying states should react in thermoneutral or exothermic processes, Table II. Indeed, analysis of the endothermic feature using eq 1, Table III, gives $E_T = 0.3 \pm 0.2$ eV and $E_D = 2.3 \pm 0.1$ eV.

Figure 6 also shows $\sigma(TiNH_2^+)$ for Ti^+ produced by EI using electron energies of 30 and 50 eV. (At 70 eV, results similar to the 50-eV cross section are obtained.) These cross sections each display endothermic and exothermic features. The exothermic features indicate that ions with $E_{el} \geq 1.1$ eV are populated in these beams. The endothermic features (which must be dominated by the a^2F state) have shapes and energy behavior comparable to $\sigma(^2X)$.

EI Beam Populations. Comparing the cross sections for formation of TiN^+, $TiNH^+$, and $TiNH_2^+$ when the Ti^+ reactant is formed by 30-eV EI with $\sigma(^2X)$ for each data channel should provide an indication of the populations of the a^2F state at this electron energy. We find relatively consistent values of 18 ± 6%, 13 ± 5%, and 10 ± 6%, respectively. Averaging these three values gives our reported a^2F population of Ti^+ beams produced by EI at 30 eV of 14 ± 5%. This is in agreement with a similar estimate by Sunderlin and Armentrout[5] of 9 ± 3%, Table II. For the 50-eV data, the TiN^+ and $TiNH_2^+$ cross sections show increases in the low-energy features compared to the 30-eV data, but the portion of the cross section associated with a^2F reaction remains virtually unchanged. Thus, the a^2F populations of these beams are approximately the same as those reported for the 30-eV beam.

Discussion

Thermochemistry. Table IV lists the bond strengths for the $Sc^+–H$, $Ti^+–H$, $Sc^+–NH_n$ ($n = 1, 2$), and $Ti^+–NH_n$ ($n = 0–2$) species derived here. Also listed are bond strengths for $Sc^+–CH_n$

(n = 2, 3), Ti^+–CH_n (n = 1–3), and neutral molecules of interest. $D°(ScH^+)$ and $D°(TiH^+)$ agree well with previous determinations, 2.48 ± 0.09 and 2.35 ± 0.11 eV, respectively.[21,23] Our TiN^+ bond strength is significantly higher than the theoretical value of 4.24 eV reported by Kunze and Harrison; however, the authors note that their absolute bond energies are generally low by about 25%.[24] Correcting their value by this factor provides an estimated bond energy of ~5.3 eV, in good agreement with our experimental result.

We can also compare our value for $D°(TiN^+)$ to the literature value for $D°(TiN)$ = 4.93 ± 0.35 eV.[25] Using these bond strengths and the ionization potential of titanium, IP(Ti) = 6.820 ± 0.006 eV,[26] allows us to calculate IP(TiN) = 6.56 ± 0.37 eV. The similarity of the IPs for Ti and TiN suggests that ionization of TiN involves the removal of an electron from a nonbonding metal orbital.

The bond energies $D°(ScNH^+–H)$ = 2.53 ± 0.12 eV, $D°(TiN^+–H)$ = 3.10 ± 0.18 eV, and $D°(TiNH^+–H)$ = 2.86 ± 0.18 eV can also be calculated form our data. $D°(TiN^+–H)$ and $D°(TiNH^+–H)$ are considerably stronger than $D°(TiH^+)$. They are somewhat weaker than $D°(N–H)$ = 3.46 eV, a result of the stabilization energy involved in forming a π bond in these molecules. Thus, these bond strengths are consistent with the Ti^+–NH and Ti^+–NH_2 structures, rather than H–Ti^+–N and H–Ti^+–NH. In contrast, $D°(ScNH^+–H)$ is almost identical with $D°(ScH^+)$, which seems to suggest that the structure for this molecule is H–Sc^+–NH. However, Sc^+ has only two valence electrons and therefore can form at most two covalent bonds. As shown below, the Sc^+–NH bond requires both of the Sc^+ valence electrons, such that a $HNSc^+$–H bond cannot be as strong as the covalent Sc^+–H bond (or alternatively, the HSc^+–NH bond cannot be as strong as the Sc^+–NH bond). Rather, the low $ScNH^+$–H bond energy is a result of the large stabilization energy (~1.5 eV, see below) involved in forming a π bond in the Sc^+–NH molecule. Thus, the most reasonable structure is believed to be Sc^+–NH_2.

One other thermodynamic result comes from the failure to observe the ScN^+ product. This is attributed to a weak Sc^+–N bond, the result of only two valence electrons on Sc^+. Indeed, Kunze and Harrison find that Sc^+–N has a doublet spin with a bond energy of 2.7 eV or, after correction, 3.4 eV. This low bond energy means that $ScNH_2^+$ decomposes preferentially by H atom loss (which requires 2.5 eV), rather than by dehydrogenation (which requires 3.2 eV). Note that the latter channel is not only thermodynamically disfavored but kinetically disfavored as well (since it must proceed via a tight transition state while H atom loss occurs via a loose transition state).

Bond Energy–Bond Order Correlation. Previously,[27] we have discussed the qualitative correlations between V^+–CH_n (n = 0–3) and CH_n–CH_n bond strengths, and recently we extended this to V^+–NH_n (n = 0–2) and NH_n–CH_n bond strengths.[1] Figure 7 shows such correlations for the Sc^+–L and Ti^+–L (L = CH_n and NH_n) systems and are directly analogous with the V^+ results. Ti^+–N agrees readily with the trend seen for the carbon ligands and falls in the region associated with covalent triple bonds. Since Ti^+ has three valence electrons, a triple bond implies that TiN^+ has no unpaired electrons and therefore should have a singlet spin state, in agreement with the calculations of Kunze and Harrison.[24]

In contrast, the M^+–NH_2 and M^+–NH bond strengths are markedly higher than their isoelectronic M^+–CH_3 and M^+–CH_2 bond strengths. Thus, the lone pair of electrons on nitrogen must be contributing to the bonding, presumably by donating into empty metal d orbitals. The end result is that $D°(M^+–NH_2)$ are nearly equivalent to the M^+–CH_2 double-bond energies and $D°(M^+–NH)$ are comparable to triple-bond energies. The bond strength enhancement due to the interaction of the N atom lone pair electrons with empty metal d orbitals is ~1.5 eV for both metal ions (as indicated by the y intercepts in the upper lines of Figure 7). In the case of V^+, this enhancement was about 1.4 eV.[1]

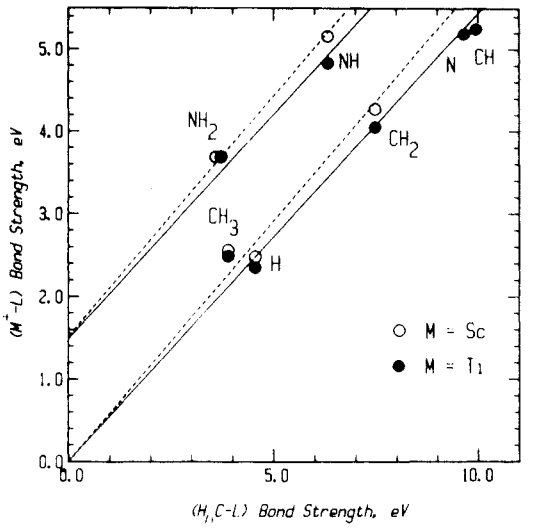

Figure 7. Bond dissociation energies from Table IV for Sc^+–L (○) and Ti^+–L (●) vs H_nC–L where L is the group indicated. The two points for M^+–NH_2 coincide. The lower lines (dashed for Sc, full for Ti) show the result of linear regression fits (slope = 0.58 for Sc and 0.54 for Ti) of the hydrocarbon data. The upper lines are the best fits to the L = NH and NH_2 data while retaining the slope of the lower lines for each metal.

Reaction Mechanism. The reaction mechanism for the interaction of V^+ with ammonia has been described in detail and is similar to that for the V^+ + methane reaction.[1] Similarly, the mechanisms for reaction of Sc^+ and Ti^+ with methane have been detailed.[4,5] These ideas are easily extended to the interaction of Sc^+ and Ti^+ with ammonia. Therefore, in this section, we briefly outline the mechanism and show how it accounts for the reaction products observed and for the reactivities of specific metal ion electronic states.

An obvious first step in a mechanism that explains the observed competition between the MH^+ and MNH_2^+ products is oxidative addition of the N–H bond at the metal center to form H–M^+–NH_2, intermediate I. Bond additivity estimates show that formation of I from reactants is ~1.5 and ~1.4 eV exothermic for M = Sc and Ti, respectively. At elevated energies, I decomposes by M–H or M–N bond cleavage to form MNH_2^+ + H or MH^+ + NH_2, respectively. MNH_2^+ is thermodynamically favored, Table IV, but at high energies, where both reactions are thermodynamically allowed, MH^+ formation dominates due to angular momentum constraints which have been detailed previously.[1,2] MN^+ and the high-energy part of $\sigma(MNH^+)$ are formed by MNH_2^+ decomposition, as discussed above.

We envision three possible mechanisms for the dehydrogenation process: 1,1-H_2 loss from intermediates II or III, or 1,2-H_2 loss from I via the four-center transition state IV. Intermediate II

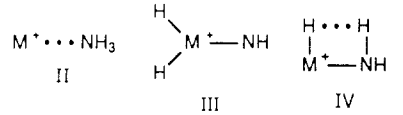

is the ion–dipole complex formed in the initial interaction of M^+ with ammonia, and III is formed by a α-H transfer from I. As in the case for V^+, we believe that the reaction proceeds via intermediate IV, since it accounts for the electronic-state dependence of the Ti^+ and V^+ reactions (discussed below) and is reasonable from a thermodynamic standpoint. Intermediate II fails to provide an easy explanation for the spin-specific reactivities of Ti^+ or V^+. Intermediate III is thermodynamically unreasonable for M = Sc, since Sc^+ has only two valence electrons, and therefore cannot support the three covalent bonds of III. Even if the Sc^+–H bonds are covalent and the H_2Sc^+–NH bond is dative, formation of III from reactants is estimated to require between 0.6 and 2 eV. For the reaction of Ti^+ with ammonia, we cannot rule out the possibility of dehydrogenation occurring via III, but the sim-

(24) Kunze, K. L.; Harrison, J. F. *J. Phys. Chem.* **1989**, *93*, 2983–2997.
(25) Stearns, C. A.; Kohl, F. J. *High Temp. Sci.* **1970**, *2*, 146.
(26) Sugar, J.; Corliss, C. *J. Phys. Chem. Ref. Data* **1985**, *14* (Suppl. No. 2).
(27) Aristov, N.; Armentrout, P. B. *J. Am. Chem. Soc.* **1984**, *106*, 4065–4066.

ilarity of the Sc^+ and Ti^+ systems argues against it. Furthermore, in the $M^+ + CH_4$ systems, the thermochemistry unambiguously favors an intermediate analogous to IV (since formation of the analogues to III is clearly too high in energy).[4,5]

Electronic-State Dependence. In order to understand why the doublet states of Ti^+ are more reactive that the quartet states, we use ideas discussed in detail for the V^+ with NH_3 system.[1] Briefly, there are two factors which couple together to govern the reaction potential energy surfaces: spin conservation and molecular orbital considerations. For the purposes of the present discussion, however, the key consideration is the spin state of intermediate I and the products. For $H-Ti^+-NH_2$, containing covalent Ti–H and Ti–N bonds, two of the three Ti^+ valence electrons are involved in bonding, leading to a doublet ground state. (Sc^+ has one fewer electron than Ti^+; thus, $H-Sc^+-NH_2$ should be a singlet.) For the product species, the bond energies discussed above strongly suggest that the M^+-NH_2 species have one covalent bond between M and N and that the M^+-NH species involve two covalent bonds. For Sc^+, with two valence electrons, this leads to a probable doublet ground state for Sc^+-NH_2 (with a single nonbonding electron on the metal) and a singlet ground state for Sc^+-NH. Presuming that the extra valence electron on Ti^+ goes into a nonbonding d orbital with high-spin coupling suggests a triplet ground state for Ti^+-NH_2 and a doublet ground state for Ti^+-NH.

We conclude from these results that reaction of $Ti^+(^4F) + NH_3$ cannot proceed via the ground state of intermediate I in a spin-conserved reaction. Further, since $TiNH^+$ also has a doublet ground state, production of $TiNH^+ + H_2$ is spin-forbidden from $Ti^+(^4F)$. (Likewise, formation of $ScNH^+ + H_2$ is spin-forbidden from the $Sc^+(^3D)$ ground state.) Consequently, reaction of the doublet states of Ti^+ is much more efficient than that of the quartet states (and presumably, the singlet states of Sc^+ are more reactive than the triplet states). We also note that the reactivity of the quartet states is much higher for dehydrogenation (a factor of $\sim$100 over an energy range of 1–3 eV) than for H or NH_2 loss (factors of $\sim$7 and $\sim$18,[28] respectively, over the same energy range). This is presumably because the dehydrogenation reaction requires a change in spin for high-spin reactants, while the latter two reactions can conserve spin starting from either quartet or doublet reactants (since TiH^+ and $TiNH_2^+$ are triplets and H and NH_2 are doublets). The fact that these reactions exhibit any sensitivity to spin is an indication that the preferred reaction pathway is via intermediate I.

We also find that the probability of the $MNH^+ + H_2$ reaction varies appreciably from metal to metal as well as state to state. The results presented here and those for the V^+ with ammonia system[1] show that the low-spin ions of Ti^+ and V^+ react at the collision limit.[29] In contrast, the low-lying high-spin states of Ti^+ and V^+ react with efficiencies of $\sim$20% and $\sim$1%, respectively, at about 0.1 eV. $\sigma(ScNH^+)$ obtained from Sc^+ produced at 2225 K (and shown to be dominated by high-spin ions) is about 40% of the collision limit. Since these reactions are exothermic with no activation barriers, the inefficiency of the high-spin states is attributed to the need to undergo the spin-forbidden surface crossing. The change in this inefficiency with metal is most easily rationalized by considering the energy splittings between the high- and low-spin states. For Sc^+ and Ti^+, Table II shows that the splitting between the ground-state high-spin and the first low-spin state is 0.30 and 0.56 eV, respectively. In V^+, this splitting is 1.07 eV.[26] Thus, as the energy splitting between the high- and low-spin states increases, the coupling efficiency between the reaction surfaces evolving from these states decreases.

Finally, we note that the energy dependences of the ^4F and ^2X cross sections for the dehydrogenation reaction differ. The former declines as $\sim E^{-2.6}$ while the latter falls off as $\sim E^{-1.4}$. Some of this difference can probably be explained by a simplified Landau–Zener model.[30] In the limit of weak coupling between the surfaces,[31] this predicts that the probability of crossing from one surface to another has an energy dependence of $E^{-0.5}$. This prediction for the difference in slopes for the ^4F and ^2X cross sections may not be quantitative because the potential energy surfaces here must be much more complex than assumed in the one-dimensional Landau–Zener approach. Such complications have been discussed previously.[32]

Summary

Both Sc^+ and Ti^+ form MH^+, MNH^+, and MNH_2^+ products upon interaction with ammonia. Ti^+ also forms TiN^+, but Sc^+ does not. Dehydrogenation of ammonia by M^+ to form MNH^+ occurs exothermically for all states of M^+, while reactions producing all other products are endothermic for reaction of ground-state M^+. For the reaction of $Ti^+ + NH_3$, excited states (largely the a^2F) are found to be between 1 and 2 orders of magnitude more reactive than the low-lying quartet states even after accounting for the differences in available energy. This is shown by the ^4F and ^2X cross sections of Figures 4–6.

The most likely reaction mechanism for the interaction of M^+ with NH_3 proceeds via oxidative addition of a N–H bond to yield I, $H-M^+-NH_2$. Simple bond cleavage of I forms the MH^+ and MNH_2^+ products, while a four-center molecular elimination of H_2 leads to the exothermic formation of the MNH^+ product. At high kinetic energies, $ScNH_2^+$ decomposes to form $ScNH^+ + H$, while $TiNH_2^+$ decomposes to $TiNH^+ + H$ and $TiN^+ + H_2$.

The reactivities of the low-lying ^4F and excited doublet states of the Ti^+ system are rationalized by using spin conversion ideas which have been useful in understanding the reactions of atomic transition metals with H_2,[21] CH_4,[5] and NH_3.[1] Since intermediate I should have a doublet spin, its formation from the doublet states of Ti^+ can occur readily. In contrast, reactions of the ^4F states of Ti^+ which pass through intermediate I must involve spin-forbidden processes. The observation that the ^4F states react to form $TiNH^+ + H_2$ demonstrates that such spin-forbidden processes must occur.

Thermochemistry of the metal hydride products is found to agree with previous results. New thermochemistry for $ScNH^+$, $ScNH_2^+$, TiN^+, $TiNH^+$, and $TiNH_2^+$ is reported and tabulated in Table IV. Comparison of these bond strengths to analogous hydrocarbon and metal–carbon species indicates that there is a significant interaction between the lone pair of electrons on nitrogen and empty metal d orbitals. This leads to a substantial increase in the metal–nitrogen bond strengths in $ScNH^+$, $ScNH_2^+$, $TiNH^+$, and $TiNH_2^+$.

Acknowledgment. This work is supported by the National Science Foundation, Grant 8917980.

Registry No. NH_3, 7664-41-7; Ti^+, 14067-04-0; Sc^+, 14336-93-7.

(28) This value was estimated by comparing $\sigma(TiH^+,SI)$ to $\sigma(TiH^+,EI\ 30\ eV)$ and correcting for the population of the a^2F state, Table II.

(29) The efficiencies cited here are based on comparison to a simple Langevin–Gioumousis–Stevenson (LGS) model for ion–molecule reactions. Since ammonia has a permanent dipole, this model cannot be quantitative but is an accurate lower limit. An upper limit can be obtained from the locked dipole (LD) approximation. These models are shown in Figure 5 and are discussed in detail in ref 1.

(30) Landau, L. D. *Phys. Z. Sowjetunion.* **1932**, *2*, 46. Zener, C. *Proc. R. Soc. London, A* **1932**, *137*, 696. Stueckelberg, E. C. G. *Helv. Phys. Acta* **1932**, *5*, 369.

(31) Burley, J. D.; Ervin, K. M.; Armentrout, P. B. *J. Chem. Phys.* **1987**, *86*, 1944–1953.

(32) Schultz, R. H.; Elkind, J. L.; Armentrout, P. B. *J. Am. Chem. Soc.* **1988**, *110*, 411–423.